

Accepted Manuscript

Synthesis, structure, DFT study and catechol oxidase activity of Cu(II) complex with sterically constrained phenol based ligand

Bikramaditya Mandal, Mithun Chandra Majee, Trilochan Rakshit, Snehasis Banerjee, Partha Mitra, Debdas Mandal



PII: S0022-2860(19)30521-6

DOI: <https://doi.org/10.1016/j.molstruc.2019.04.110>

Reference: MOLSTR 26482

To appear in: *Journal of Molecular Structure*

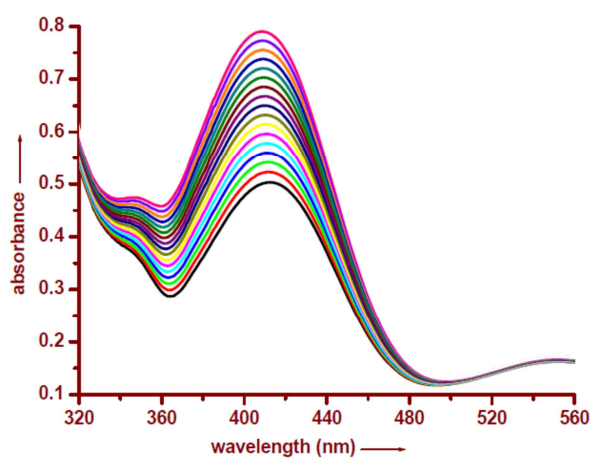
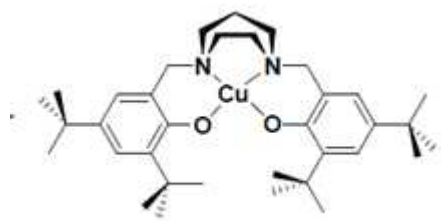
Received Date: 17 December 2018

Revised Date: 22 April 2019

Accepted Date: 25 April 2019

Please cite this article as: B. Mandal, M.C. Majee, T. Rakshit, S. Banerjee, P. Mitra, D. Mandal, Synthesis, structure, DFT study and catechol oxidase activity of Cu(II) complex with sterically constrained phenol based ligand, *Journal of Molecular Structure* (2019), doi: <https://doi.org/10.1016/j.molstruc.2019.04.110>.

This is a PDF file of an unedited manuscript that has been accepted for publication. As a service to our customers we are providing this early version of the manuscript. The manuscript will undergo copyediting, typesetting, and review of the resulting proof before it is published in its final form. Please note that during the production process errors may be discovered which could affect the content, and all legal disclaimers that apply to the journal pertain.



Synthesis, structure, DFT study and catechol oxidase activity of Cu(II) complex with sterically constrained phenol based ligand

Bikramaditya Mandal ^a, Mithun Chandra Majee ^b, Trilochan Rakshit ^a, Snehasis Banerjee ^c, Partha Mitra ^b, Debdas Mandal ^{a,*}

^a Department of Chemistry, Sidho-Kanho-Birsha University, Purulia - 723104, West Bengal, India.

^b Department of Inorganic Chemistry, Indian association for the cultivation of science, Kolkata – 700032, India.

^c Department of Chemistry, Govt. College Of Engineering and Leather Technology, Salt Lake Sector-III, Block-LB, Kolkata- 700106, India

* *Corresponding author* E mail – id: deb_mandal@yahoo.co.in (Debdas Mandal)

Abstract

A mononuclear Cu(II) complex $[\text{Cu}^{\text{II}}(\text{L})](\mathbf{1})$ [$\text{H}_2\text{L}=\text{N},\text{N}'\text{-bis(2-hydroxy-3,5-di-tert-butylbenzyl)-homopiperazine}$] has been synthesized by using sterically constrained tetradentate phenol-based ligand. Characterization of this compound has been carried out by various spectroscopic tools. Compound **1** crystallizes in orthorhombic space group $P2_12_12_1$ with $a = 9.9794$ Å, $b = 11.944$ Å, $c = 28.719$ Å. Single crystal X-ray diffraction study reveals that in mono nuclear copper(II) complex $[\text{Cu}^{\text{II}}(\text{L})]$ **1**, the metal center adopts a square planar environment. The geometry of the Cu(II) complex has been optimized using density functional theory (DFT) calculations. Electronic excitation energies of the above mentioned complex are calculated by TDDFT/UB3LYP method combined with the SMD solvation in methanol medium. Electrochemical nature of the bis phenol based copper complex confirms that both the oxidation process ($E_{1/2} = 0.56$ V and $E_{1/2} = 0.89$ V) arise due to ligand based oxidation of the phenol moiety to phenoxyl radical. Compound **1** acts as an effective catalyst towards the oxidation of 3,5-di-tert-butylcatechol in methanol solvent to its corresponding quinone derivative in aerial oxygen. The kinetic parameters have been determined using Michaelis–Menten approach. The K_{cat} value for **1** in methanol is 722 h^{-1} .

Keywords: *Syntheses, Characterization, X-ray structure. DFT study, Catecholase activity.*

1. Introduction

Metalloenzyme containing copper ions at their active site are usually involved in a range of biological processes, such as electron transfer or oxidation of organic substrates [1]. The ability of copper proteins to reversibly bind dioxygen at ambient conditions has inspired numerous research groups to study their structural, spectroscopic and catalytic properties [2]. Catechol oxidase is an enzyme with a type-3 di-copper active site that catalyzes the oxidation of a range of ortho-diphenol (catechol) substrates to the corresponding ortho-quinones. The generated o-quinones are auto polymerized producing a brown polyphenolic pigment, i.e., melanin, a process which is considered to protect damage tissues against pathogens or insects [3]. In 1998, X-ray crystallographic characterization of catechol oxidase, isolated from sweet potatoes, was reported. The reported results reveals that the active center consists of a hydroxo-bridged dicopper(II) center in which each copper(II) center is coordinated to three histidine nitrogens and adopts a trigonal pyramidal environment with one nitrogen at the apical site [4]. The ability of di-copper complexes to oxidize phenols and catechols is well established from the report of various research groups [5]. Several monocopper (II) complexes are also known to exhibit catecholase activity [6]. There are different approaches used in the literature to study the mechanism of the catalytic oxidation of the substrate (catechol) by these compounds. There are several model system follow the pathway which produces two molecules of quinone and water [7]. At the same time many complexes oxidise catechol through an alternate pathway which involves the production of quinone along with H_2O_2 rather than water [8].

Herein, we prepare mononuclear square planar Cu(II) complex for $[\text{CuL}]$ (**1**) with redox active di-tertiary butyl substituted phenol based tetradentate N_2O_2 ligand. X-ray crystallography, electronic spectroscopy and ESI- MS have been carried out to characterize this complex. The electrochemical studies of **1** show two reversible oxidation peaks in the positive potential range due to the ligand centered redox processes in which phenolate group yields phenoxyl radical in this complex.

Furthermore, the copper complex **1** is found to be an effective functional model of the enzyme as it catalyzes the oxidation of 3,5-di-tert-butylcatechol (3,5-DTBC) to 3,5-di-tert-butylbenzoquinone (3,5-DTBQ) with molecular oxygen in methanol at 25°C.

2. Experimental section

2.1. Materials

Homopiperazine, 2,4-di-tert-butylphenol and 3,5-di-tert-butylcatechol were purchased from Aldrich. Solvents were reagent grade, purified using appropriate drying agents and distilled under nitrogen prior to their use [9]. All other chemicals were commercially available and were of reagent grade and used as received without further purification.

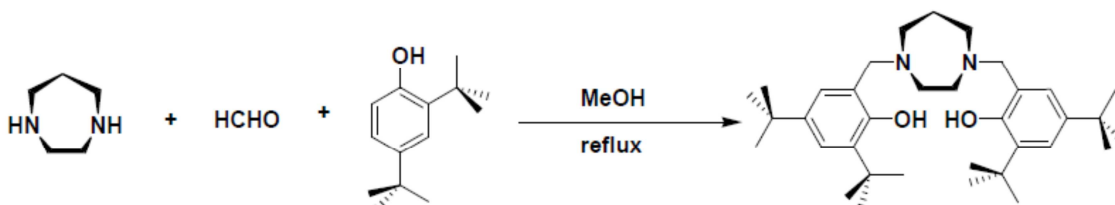
2.2. Synthesis

2.2.1. Ligand

N,N'-bis(2-hydroxy-3,5-di tertiarybutylbenzyl)-homopiperazine (**H₂L**) Homopiperazine (1.0 g, 10 mmol) was taken in methanol (50 mL). To the methanolic solution about 0.60 g (20 mmol) of paraformaldehyde was added. The resulting solution was refluxed for 3 h. To this 2,4-di-tert-butylphenol (4.12 g, 20 mmol) was added slowly with constant stirring. The resulting mixture was refluxed further for 12 h to obtain a white crystalline precipitate which was filtered off, washed with methanol (2 × 10 mL) and diethyl ether (2 × 10 mL) and finally dried in vacuum. The compound was recrystallized from acetone-pet ether (60–80°C) mixture. Yield: 4.28 g (80 %). Anal. Calcd. for C₃₅H₅₆N₂O₂: C, 78.31; H, 10.51; N, 5.22. Found: C, 77.92; H, 10.20; N, 5.02.

¹H NMR (300 MHz, CDCl₃, 25°C), δ/ppm: 1.32 (s, 18H, CH₃), 1.38 (s, 18H, CH₃), 1.97 (s, 2H, -CH₂-), 2.77 (s, 4H, N-CH₂-), 2.83 (s, 4H, CH₂-CH₂), 3.77 (s, 4H, benzylic), 6.82 (s, 2H, aryl), 7.21 (s, 2H, aryl).

IR (KBr disk, cm⁻¹): 2956, 2904, 1481, 1434, 1360, 1236, 1164, 1093, 877, 812, 723.



Scheme 1. Schematic presentation of preparation of ligand.

2.2.2. Preparation of complex

[CuL] (**1**) Cu(OAc)₂·2H₂O (0.1 g, 0.5 mmol) was added to the methanol solution of H₂L (0.27g, 0.5 mmol) and the resulting mixture was stirred. After 1h stirring, solution was turned into dark color. Resulting solution was filtered. The filtrate was kept undisturbed in open air at room temperature for crystallization. After 1 day, brown crystalline compound along with single crystals was obtained. IR (KBr disk, cm⁻¹): 2952, 2855, 1464, 1436, 1366, 1306, 1257, 1167, 1146, 827, 736, 526. Anal. Calcd. for C₃₅H₅₄CuN₂O₂: C, 70.25; H, 9.10; N, 4.68. Found: C, 70.10; H, 8.88; N, 4.21. UV-Vis (CH₂Cl₂), [λ_{\max} /nm (ϵ /mol⁻¹cm²): 422 (1351), 550(848). ESI-MS in CH₂Cl₂: m/z (M+H⁺): 598.

2.3. Physical measurements

UV-visible spectra in solution were recorded on a Perkin-Elmer 950 UV/VIS/NIR spectrophotometer, while for infrared spectra were employed a Nicolet Magna 750 FT-IR spectrometer, series II with samples prepared as KBr pellets. Mass spectra (ESI-MS in positive ion mode) were recorded on a QTOF Model YA263 Micro Mass Spectrometer. The electrochemical measurements were carried out with a BAS epsilon electrochemistry system. A three-electrode assembly comprising a Pt (for oxidation) or glassy carbon (for reduction) working electrode, Pt auxiliary electrode and Ag/AgCl reference electrode were used. The cyclic voltammetric study (CV) was carried out at 25°C in CH₃CN solution of the complex (*ca.* 1 mM) and the concentration of the supporting electrolyte tetraethylammonium perchlorate (TEAP) was maintained at 0.1 M. All of the potentials reported in this study were referenced against the Ag/AgCl electrode, which under the given experimental conditions gave a value of 0.36 V for the ferrocene/ferrocenium couple.

2.3.1. X-ray crystallography

Diffraction quality crystals of **1** were grown at room temperature by slow diffusion of methanol solution of the compound. Intensity data for the compound was measured on a Bruker SMART 1000 CCD diffractometer using a graphite monochromatic Mo K α radiation (λ = 0.71073 Å) at 293 K. Intensity data were collected with θ_{\max} of 25 deg. No crystal decay was observed during the data collections. Relevant crystal data and refinement details are given in Table 1. The structures

were solved by direct methods [10] and refined on F^2 by a full-matrix least-squares procedure [11] using the program SHELXL 97.

Table 1 Summary of the Crystallographic Data for the Complex **1**.

Empirical formula	C ₃₅ H ₅₄ Cu N ₂ O ₂
Formula weight	598.34
T (K)	293 (2)
λ (Mo K α), Å	0.71073
Space group	P2₁2₁2₁
Crystal system	orthorhombic
a (Å)	9.9794
b (Å)	11.944
c (Å)	28.719
V (Å ³)	3423
Z	4
$D_{\text{Calcd.}}$ (g cm ⁻³)	1.161
μ (mm ⁻¹)	0.668
$F(000)$	1292
θ ranges (°)	1.42 – 25.00
Index ranges	$-11 \leq h \leq 9$
	$-13 \leq k \leq 14$
	$-34 \leq l \leq 33$
Reflections collected	25114
R_{int}	0.0949
Goodness of fit	1.032
No. of parameters	373
$RI^a(F_o)$, $wR2^b(F_o)$ (all data)	0.0599, 0.1306
Largest diff. peak, deepest hole (eÅ ⁻³)	0.621, -0.347

$$^a R = \sum ||F_o| - |F_c|| / \sum |F_o|, \quad ^b wR = [\sum [w((F_o^2 - F_c^2)^2)] / \sum w(F_o^2)^2]$$

2.3.2. Theoretical methods

All of the molecular parameters needed in this paper are calculated by unrestricted density functional theory (DFT) using Gaussian 09 program [12]. The geometries are optimized by B3LYP functional starting from the X-ray crystallographic data [13]. This functional was combined with the 6-31G(d,p) atomic basis set for all first and second-row atoms. Relativistic effects were included for Cu atom using LANL2DZ pseudopotential [14]. The nature of the stationary points was confirmed by computing the Hessian at the same level of theory. To explore the absorption spectral properties for the investigated complex, the time-dependent density functional theory (TD-DFT) was adopted on the basis of the optimized ground state of doublet state.

2.3.3. Catalytic oxidation of 3,5-DTBC

The catecholase activity of complex **1** was monitored using most familiar 3,5-di-tertbutylcatechol (3,5-DTBC) as the substrate in a methanol solution under aerobic conditions at room temperature [15]. In order to check the catechol oxidase activity of the complex, a 10^{-4} M solution of **1** in methanol solvent was mixed with 100 equiv. of 3,5-di-tertbutylcatechol (3,5-DTBC) under aerobic conditions at room temperature. The reaction was carried out spectrophotometrically by observing the increase in the maximum absorbance of the quinone band around 400 nm as a function of time [16]. Absorbance vs. wavelength of the solution was recorded at a regular time intervals of 5 min. It may be noted here that a blank experiment without catalyst does not show formation of the quinone up to 6 h in MeOH. To determine the dependence of rate on substrate concentration and upon various kinetic parameters, 1.75×10^{-4} M solution of complex **1** was mixed with increasing amounts of 3,5-DTBC from 1.4×10^{-3} M to 5×10^{-3} M. In each case, the reaction was monitored spectrophotometrically by watching the increase in the absorbance at 400 nm up to 6 hr. The rate constant versus substrate concentration data were then analyzed on the basis of the Michaelis–Menten approach of enzymatic kinetics to get the Lineweaver–Burk plot as well as the values of the parameters V_{\max} , K_M , and K_{cat} .

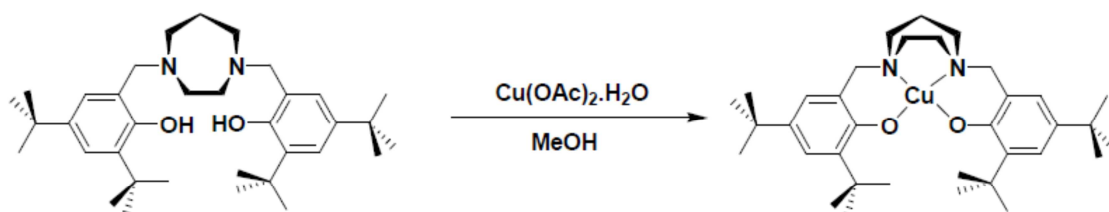
2.3.4. Detection of Hydrogen Peroxide in the Catalytic Reactions

Detection of H_2O_2 was observed by modified iodometric method during catalytic reaction [17]. The reaction mixture of catalyst and 3,5 DTBC was prepared as in the kinetic experiments. After 1 h of reaction, equal volume of water was added to the reaction mixture. The quinone was extracted from the reaction mixture by using dichloromethane. Few drops of H_2SO_4 is mixed with aqueous extract to stop further oxidation. 1 mL of a 10% solution of KI and three drops of 3% solution of ammonium molybdate were added to the reaction mixture. Hydrogen peroxide obtained from catalytic reaction oxidizes I^- to I_2 . In presence of excess iodide ions, the tri- iodide ion is produced according to the reaction $\text{I}_2(\text{aq}) + \text{I}^- \rightarrow \text{I}_3^-$. The reaction rate increases with increasing concentrations of acid and the addition of an ammonium molybdate solution condenses the reaction almost immediately. The formation of I_3^- was detected by UV – vis spectroscopy due to the development of the characteristic I_3^- band.

3. Results and Discussion

3.1. Syntheses

The copper complex has been prepared readily by mixing the copper acetate with the methanolic solution of sterically hindered phenol based N₂O₂ ligand in stoichiometric amounts (1:1 mole ratio). The detailed strategy is described in scheme 2. Mononuclear compound [Cu^{II} L] (**1**) was obtained with nearly square planar geometry and the compound is stable in air at room temperature. The compound was characterized using IR, UV–VIS spectroscopy, mass spectroscopy and single crystal X-ray crystallography. The complex was initially characterized by IR spectroscopy. IR spectra of this complex display all the characteristic bands of the coordinated L²⁻ ligand [18]. One such prominent band appears at 1257 cm⁻¹ due to ν(c-o/phenolate) stretching vibrations [19].



Scheme 2. Schematic presentation of preparation of complex 1.

3.2. Description of crystal structure

The molecular structure of complex **1** is shown in Fig.1. Its important inter atomic parameters are listed in Table 2. The complex crystallizes in orthorhombic space group $P2_12_12_1$. The Cu(II) center in this mononuclear complex is four-coordinated using a doubly deprotonated tetradentate ligand L^{2-} , providing O(1), N(1), N(2) and O(2) donor sites. The bond distances of Cu–N (2.020(5) – 2.041(4) Å) and Cu–O (1.883(4) – 1.898(3) Å) are all in the expected ranges [20]. There is no hydrogen bonding interaction present within the molecule, as well as no ion dipole interaction is present. This will also be supported from the theoretically obtained results as discussed later. Addison and Reedijk's define the geometric parameter (τ) as an index of the degree of trigonality, within the structural continuum between trigonal bipyramidal and rectangular pyramidal which is applicable to five-co-ordinate structures [21]. Yang et. al propose a very simple geometry index for four-

coordinate complexes, τ_4 , which can be used to quantify the geometry of four-coordinate species [22]. The equation is as follows

$$\tau_4 = \frac{360^\circ - (\alpha + \beta)}{141^\circ}$$

Where α and β are the two largest θ angles in the four-coordinate species. Using the above mentioned equation the magnitude τ_4 value for this copper compound is 0.143.

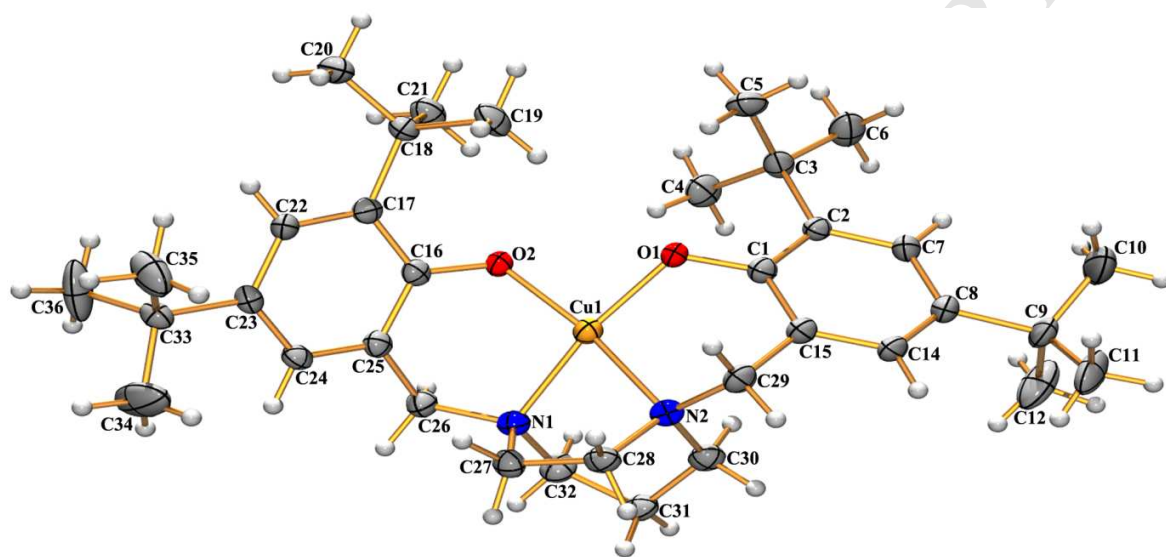


Fig. 1. Molecular structure of the complex **1** showing the atom-numbering scheme.

Table 2 Selected Bond Distances (Å) and Angles (deg) for **1**.

Bond distances (Å)		Bond angles (deg)	
Cu-O(1)	1.883(4)	O(1)-Cu-O(2)	93.35(16)
Cu-O(2)	1.898(3)	O(1)-Cu-N(1)	170.27(18)
Cu-N(1)	2.020(5)	O(2)-Cu-N(1)	94.82(18)
Cu-N(2)	2.041(4)	O(1)-Cu-N(2)	93.99(18)
		O(1)-Cu-N(2)	169.54(18)
		N(1)-Cu-N(2)	78.6(2)

3.3. Electronic spectra

The electronic spectra of the complex **1** have been observed in methanol solution of the compound at room temperature and the data are represented in the experimental section. The electronic spectrum of the copper complex shows bands at 422 nm and 550 nm which can be assigned to ${}^2B_{1g} \rightarrow {}^2A_{1g}$ and ${}^2B_{1g} \rightarrow {}^2E_{1g}$ transitions as displayed in Fig. 2 [23-24]. Remaining band maxima appearing around at UV region are due to ligand internal transition.

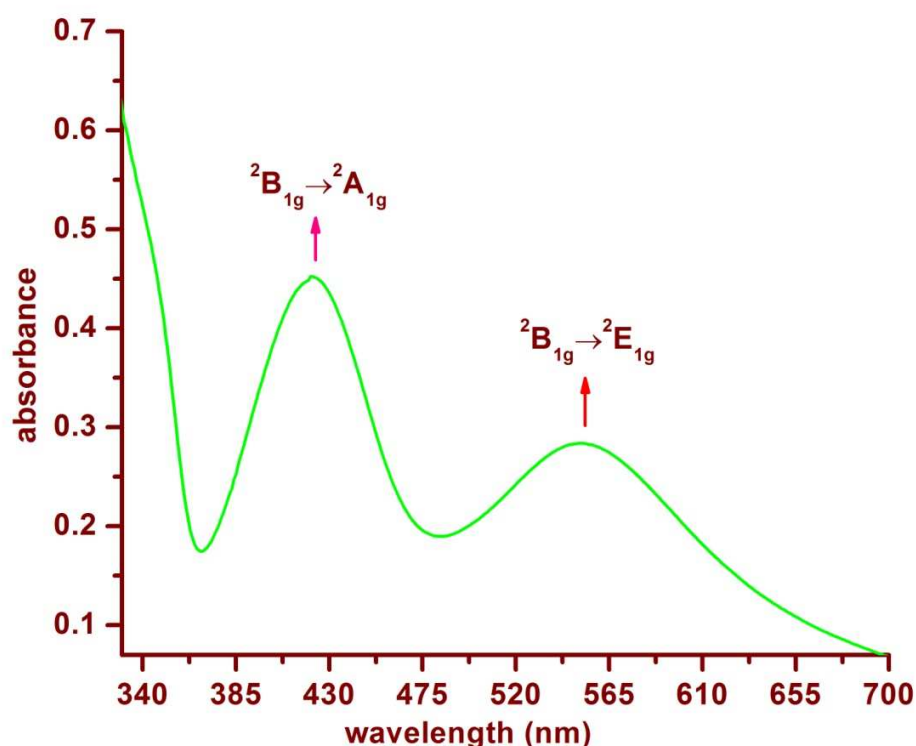


Fig. 2. Electronic absorption spectrum of complex **1** in MeOH

3.4. Electrochemical studies

The redox behavior of the complex has been examined by cyclic voltammetry in acetonitrile solution (0.1 M TBAP). Compound display main features in the potential range 0.2 V to +1.4 V vs Ag/AgCl reference as shown in Fig.3. The electrochemical studies reveal that there are two

reversible oxidation peaks for [CuL] **1** complex in the positive potential range. The first reversible electrochemical process appeared at $E_{1/2}^1 = 0.56$ V and the second reversible process at $E_{1/2}^2 = 0.89$ V. These redox processes are probably attributed to the ligand centered redox processes in which phenolate group yields phenoxyl radical in the complex [25]. Such type of observation has been reported previously in other complexes containing tertiary butyl substituted phenol based ligand [26].

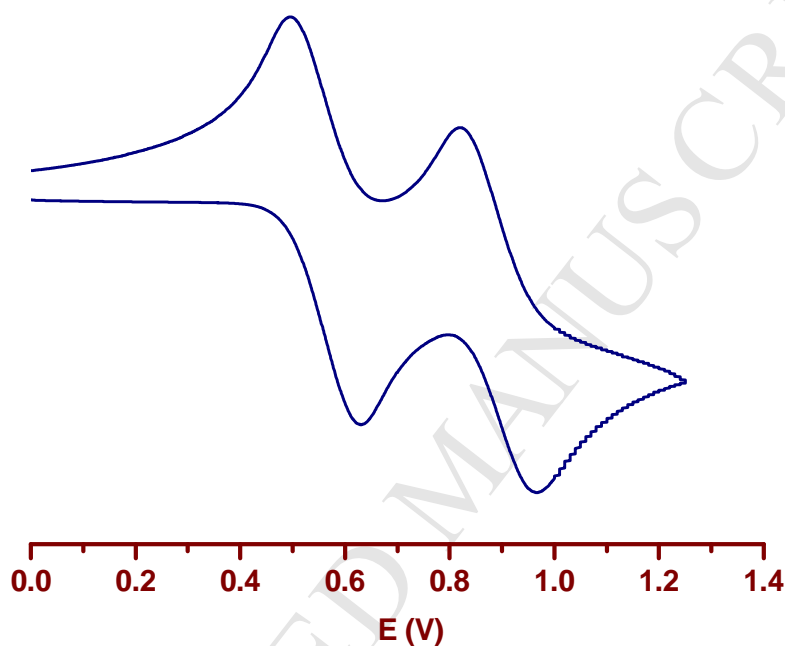


Fig. 3. Cyclic voltammograms of complex **1** in CH₃CN / 0.1 M tetraethylammonium perchlorate (TEAP) with platinum as the working electrode and saturated Ag/AgCl as the reference electrode.

Comparison of the electrochemical nature of complex **1** with related copper complexes suggests that both the oxidation processes arise due to ligand based oxidation of the phenol. For example, $\{[(3\text{-}tert\text{-butyl}5\text{-methyl}2\text{-hydroxybenzyl})(3\text{'-}tert\text{-butyl}5\text{'-methyl}2\text{'-oxobenzyl})(2\text{-pyridylmethyl})]\text{amine}\}/\text{Cu}(\text{OAc})$ exhibited two electrochemical processes in the anodic region on the CV timescale. The first quasi-reversible electrochemical process appeared at $E_{1/2} = 0.72$ V [0.21 V vs Fc/Fc^+] and the second quasi-reversible process at $E_{1/2} = 1.10$ V [0.60 V vs. Fc/Fc^+] [25a]. Apart from these structural analogues, copper bis-phenolate complex namely (*N*-benzyl-bis-*N,N'*-salicylidene)-*cis*-1,3,5-

triaminocyclohexane copper(II) showed two reversible one electron oxidations at $E_{1/2} = 0.89$ V (0.34 V vs Fc/Fc⁺) and $E_{1/2} = 1.13$ V (0.58 V vs. Fc/Fc⁺) [27].

In our cases, redox couples are ascribed to the formation of mono- and di-radical species according to following pathway.



Oxidation of one phenolate moiety into a phenoxyl radical does influence significantly the redox potential of second oxidation of the another phenolate moiety to phenoxyl radical as reported analogues, copper bis phenolate complex [28].

3.5. Theoretical study

In this study, the geometries of ground state for the title complex were optimized by means of unrestricted density functional theory (DFT) without any symmetry constraints. The best agreement with experimental results were observed for the title complex at UB3LYP/6-31G (d,p) levels. These results confirm that the complex has distorted square planar geometry as obtained in the X-ray data. In this geometry, two Cu–N bond distances are 2.11 Å and Cu–O bond distances are about 1.92 Å. The well agreement with the X-ray data (Cu–N ~2.04 Å and Cu–N ~1.89 Å) verified the reliability the theoretical methods used here.

The title complex has a spin doublet ground state. The data of frontier molecular orbital (FMO) analysis in terms of energies are shown in Table S1 and Fig. 4. A larger HOMO-LUMO gap of 4.46 eV indicates a very stable nature of the investigated complex. In order to reduce the computational cost for this large molecule, some methyl groups were excluded from the complex in the excitation process as shown in Fig. S1. On the basis of optimized ground state geometry, the TDDFT/UB3LYP method combined with the SMD solvation in methanol medium was used to calculate the absorption properties of the investigated complexes. The most important excited states, their oscillator strengths, dominant orbital excitations, and their assignments are shown in Table 3. In Fig.5 the normalized absorption spectra obtained theoretically along with the experimental spectra are shown. The simulated curve is in good agreement with that of experimentally obtained curve, however, some transitions that are found theoretically are not present in the simulated results.

A larger HOMO-LUMO energy gap (4.46 eV) for the α -MOs compared to energy β -MOs (2.1 eV) obviously indicate the low energy electronic excitations are from β -MOs. FMO analysis (Table 3) shows that, for **1**, the lowest-lying absorption at 557 nm mainly originates from β -H-2 $\rightarrow\beta$ -LUMO. This absorption band is close to the experimentally obtained band at 570 nm. The other important strong bands at 466 nm come mainly from β -H-5 to β -LUMO with the other contributions from β -H-10 and β -H-6 to β -LUMO. Slightly higher energy transition at 344 nm mainly originates from α -HOMO and α -H-2 to the α -LUMO. This band can be correlated with the assigned experimentally obtained band at 330 nm which is slightly red shifted by about 14 nm. The strong absorption at 286 nm is in excellent agreement with the experimentally obtained band at 288 nm. This band is contributed from α -HOMO to α -LUMO.

Table 3 Selected calculated wavelength (nm)/energies (eV), oscillator strength (*f*), major contribution and the experimental wavelength (nm) for the investigated complexes. H indicates HOMO, L indicates LUMO.

Complex	λ/E		<i>f</i>	configuration	Expt. (nm)
1	557	2.22	0.004	β -H-2 $\rightarrow\beta$ -LUMO (63%), β -HOMO \rightarrow LUMO (11%)	570
	466	2.66	0.019	β -H-10 $\rightarrow\beta$ -LUMO (10%), β -H-6 $\rightarrow\beta$ -LUMO (10%), β -H-5 $\rightarrow\beta$ -LUMO (36%)	450
	418	2.96	0.005	β -H-4 $\rightarrow\beta$ -LUMO (92%)	
	344	3.6	0.082	α -H-1 $\rightarrow\alpha$ -LUMO (12%), α -H-1 \rightarrow L+4 (10%), α -HOMO $\rightarrow\alpha$ -LUMO (11%), β -H-1 $\rightarrow\beta$ -L+1 (11%)	330
	286	4.33	0.032	α -HOMO $\rightarrow\alpha$ -LUMO (65%)	288

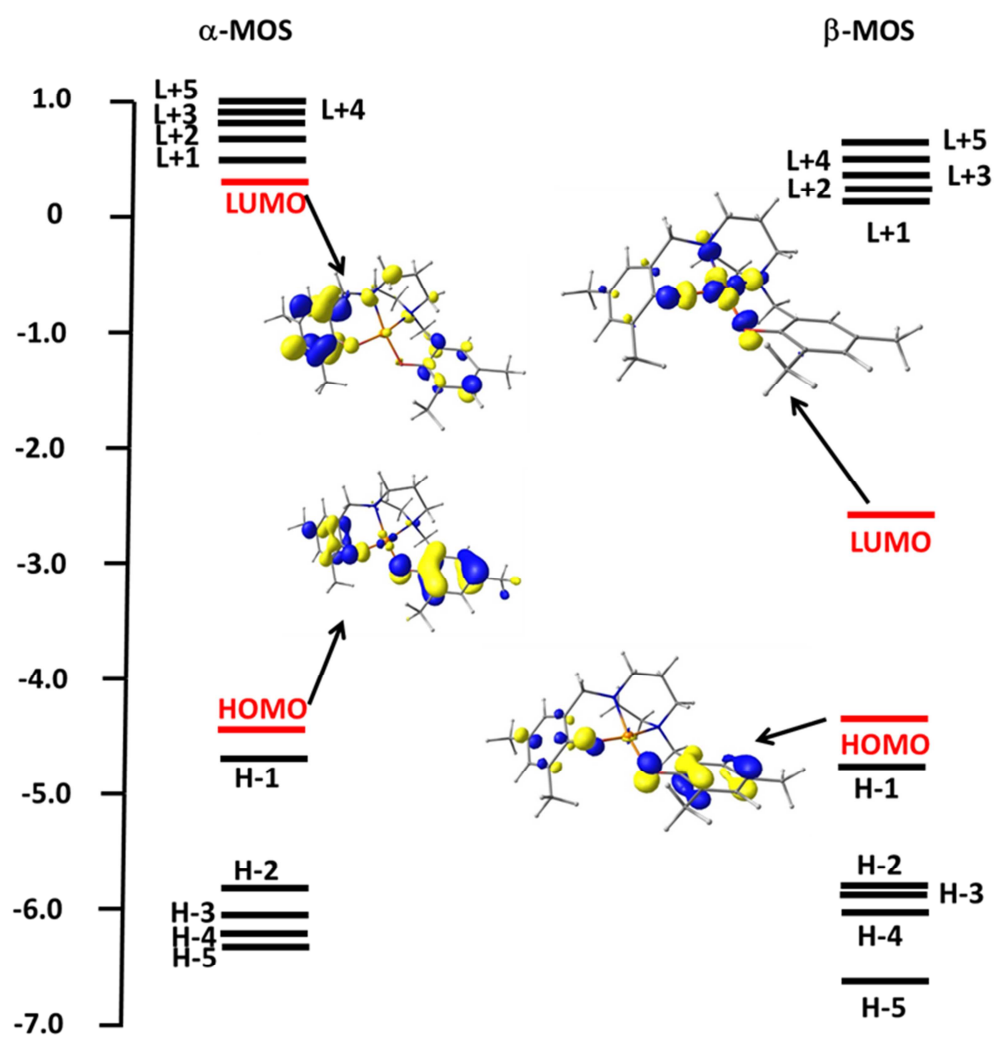


Fig. 4. Energy level energy gaps (in eV) of the FMOs for the complex 1.

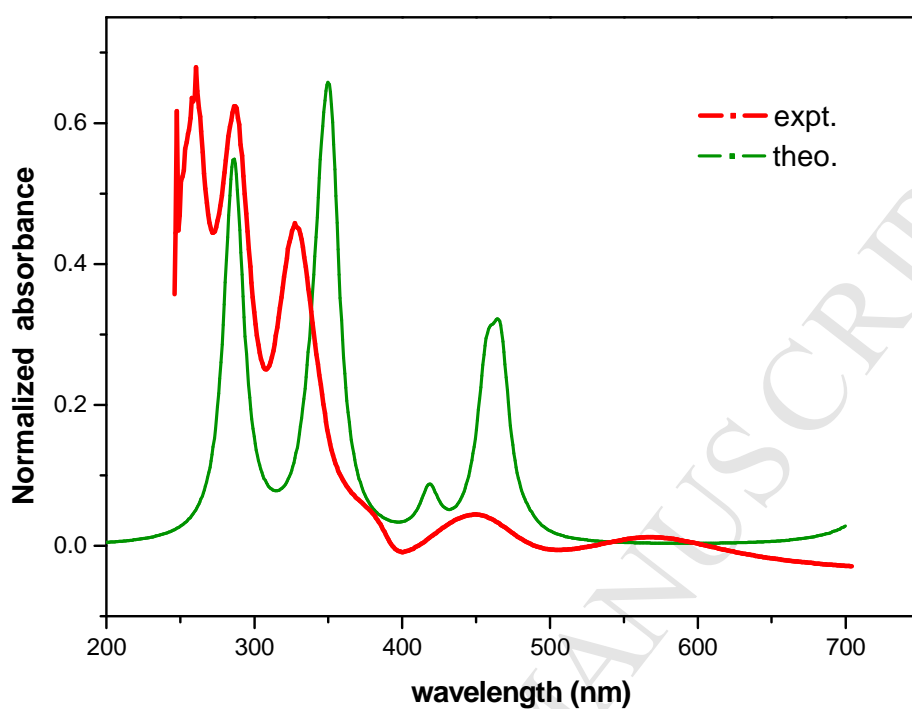


Fig. 5. Normalized simulated and experimental absorption spectra of the investigated complex.

3.6. Catecholase activity

The catechol oxidase activity of mononuclear copper complex $[\text{Cu}^{\text{II}}\text{L}]$ (**1**) was monitored using 3,5-di-tert-butyl catechol (3,5-DTBC) as a model substrate in methanol under aerobic condition at room temperature. With addition of 3,5-di-tert-butyl catechol in methanolic solution of the complex in presence of air, there was a gradual increase in absorbance at 400 nm as shown in Fig.6. characteristic to the formation of 3,5-di-tert-butyl benzoquinone. Most widely used 3,5-di-tert-butylcatechol (3,5 - DTBC) has been chosen as the substrate as it can easily be oxidised to 3,5-di-tert-butyl benzoquinone (3,5 - DTBQ). Two bulky substituents on the catechol ring makes it easily oxidizable to the corresponding o-quinone 3,5-DTBQ and shows a maximum absorption at 400 nm in methanol [15-16]. Kinetic experiments were performed spectrophotometrically with complex **1** and the substrate 3,5-DTBC in methanol at 25°C. The conversion of 3,5-DTBC to 3,5-DTBQ (Quinone band maxima) was observed with time at a wave length of 400 nm for $[\text{Cu}^{\text{II}}\text{L}]$ (**1**) in methanol. The rate constant for a particular complex–substrate concentration ratio was obtained by change in absorbance versus time plot by choosing initial rate method.

The substrate concentration dependence of the oxidation rate was watched under aerobic conditions using 1.75×10^{-4} M solution of complex **1** and increasing amounts of 3,5-DTBC from 1.4×10^{-3} M to 5×10^{-3} M. The rate constant versus substrate concentration data were explained on the basis of the Michaelis–Menten approach of enzymatic kinetics to get the Line weaver–Burk plot as well as the values of the parameters V_{max} , K_{M} , and K_{cat} . The observed rate vs. [substrate] plot in methanol solution, as well as Line weaver–Burk plot, is given in Fig.7. The V_{max} value is $5.798 \times 10^{-5} \text{ M s}^{-1}$ (Std. error 1.195×10^{-4}) whereas K_{M} value is $11.83 \times 10^{-3} \text{ M}$ (Std. error 7.546×10^{-3}). The mononuclear Cu(II) complex showed high turnover number (722 h^{-1}) for the catalytic oxidation of 3,5-DTBC to 3,5-DTBQ under mild conditions by molecular oxygen and the existence of 3,5-DTBQ was identified from ESI-MS⁺ (m/z) study (Fig. 8).

Table 4 Kinetic parameters for the oxidation of 3,5-DTBC catalyzed by **1**.

Solvent	V_{max} (M min^{-1})	Std. error	K_{M} (M)	Std. error	k_{cat} (h^{-1})
MeOH	6.74×10^{-3}	12.55×10^{-3}	1.17×10^{-2}	2.55×10^{-3}	722

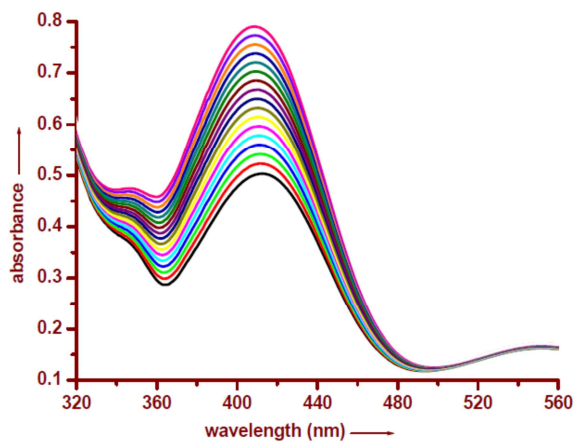


Fig.6. Increase of quinone band at 400 nm after addition of 100 equivalents of 3,5-DTBC to a solution containing complex **1** (10^{-4} M) in methanol at 25 °C.

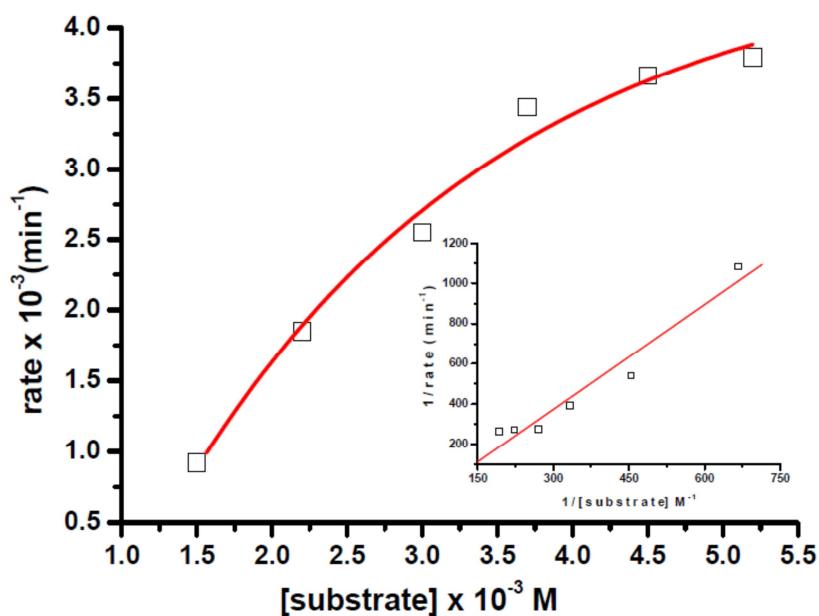


Fig. 7. Plot of rate vs. [substrate] in the presence of **1** in MeOH; inset: Lineweaver–Burk plot.

Table 5 Comparison of K_{cat} value for the oxidation of 3,5-DTBC to 3,5-DTBQ by different copper complexes

Complex	Solvent	$V_{\text{max}}(\text{M min}^{-1})$	$K_{\text{M}}(\text{M})$	$K_{\text{cat}}(\text{h}^{-1})$	Ref.
$[\text{Cu}(\text{H}_2\text{L}^{\text{a}})(\text{HL})]\text{ClO}_4$	methanol	151.8×10^{-4}	2.62×10^{-3}	9.11×10^3	29
$[\text{Cu}(\text{H}_2\text{L}^{\text{a}})(\text{HL})\text{Cu}(\text{L})]^+$	methanol	346.2×10^{-4}	1.20×10^{-3}	2.08×10^4	29
$[\text{Cu}(\text{L}^{2\text{a}})(\text{NO}_3)_2]$	methanol	2.83×10^{-5}	1.2×10^{-3}	3	30
$[\text{Cu}(\text{L}^{2\text{b}})(\text{NO}_3)_2]$	methanol	3.59×10^{-5}	2.7×10^{-2}	6	30
$[\text{Cu}(\text{dicl})_2(2\text{-pic})_2]$	methanol	2.35×10^{-4}	6.91×10^{-6}	140.04	31
$[\text{Cu}(\text{dicl})_2(4\text{-pic})_2]$	methanol	1.69×10^{-4}	9.84×10^{-5}	101.16	31
$[\text{Cu}(\text{dicl})_2(2\text{-ampy})_2]$	methanol	1.59×10^{-4}	3.44×10^{-5}	95.04	31
$[\text{Cu}_2(\text{H}_2\text{bbppnol})(\mu\text{OAc})(\text{H}_2\text{O})_2]\text{Cl}_2 \cdot 2\text{H}_2\text{O}$	methanol	144×10^{-7}	7.9×10^{-4}	28.44	32
$[\text{Cu}^{\text{II}}_2(\text{L}^3\text{-O})(\text{OH})(\text{OClO}_3)_2] \cdot 1.5\text{H}_2\text{O}$	methanol	15×10^{-6}	0.40×10^{-3}	36	33
$[\text{Cu}_2\text{L}^4_2(\text{ClO}_4)_2]$	methanol	1.56×10^{-4}	3.32×10^{-3}	93.6	34
Complex 1	methanol	6.74×10^{-3}	1.17×10^{-2}	722	Present work

Where $\text{H}_2\text{L}^{\text{a}}$ = Pyridine-2,6-dimethanol, $\text{L}^{2\text{a}}$ = N-(2,6-diethylphenyl)-2-[(pyridin-2-ylmethyl)amino]acetamide, $\text{L}^{2\text{b}}$ = N-(mesityl)-2-[(pyridin-2-ylmethyl)amino]acetamide, Diclofenac = Hdicl = 2-(2,6-dichloroanilino)phenylacetic acid), 2-pic = 2-picolin, 4-pic = 4-picoline, 2-ampy = 2-aminopyridine, $\text{H}_3\text{-bbppnol}$ = N,N'-bis(2-hydroxybenzyl)-N,N'-bis-(pyridylmethyl)]-2-hydroxy-1,3-propanediamine, $\text{L}^3\text{-OH}$ = 1,3-bis[(2-dimethylaminoethyl)iminomethyl]phenol, HL^4 = 2-[[2-(diethylamino)-ethylamino]methyl]phenol.

Table 5 shows the catalytic activities of some mononuclear Cu(II) as well as some multi nuclear Cu(II) complexes. It is worth mentioning that our complex showed quite high TON (K_{cat}) for the catalytic oxidation of 3,5 DTBC to 3,5 DTBQ by comparing with other reported work [29 -34].

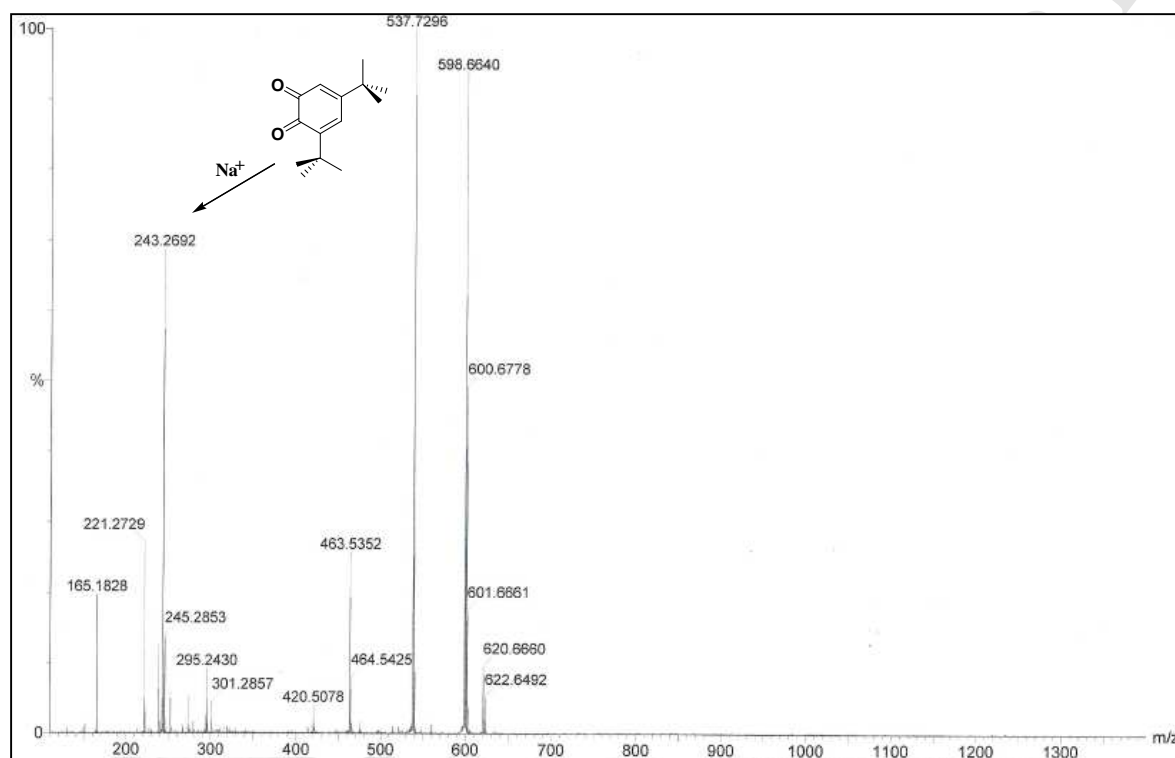
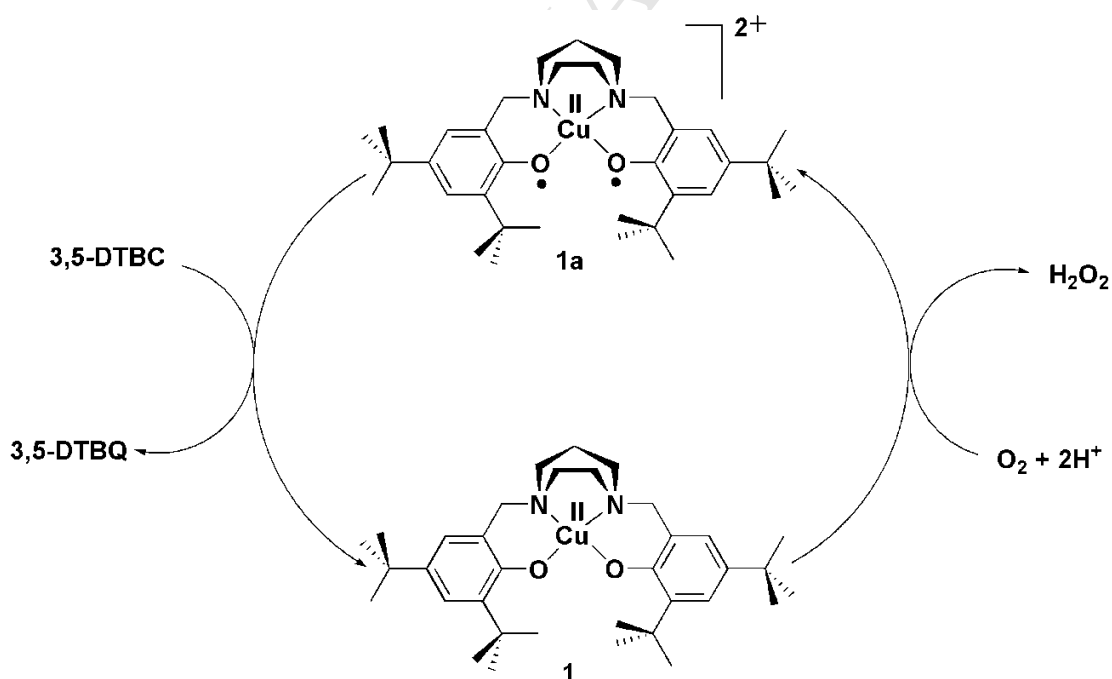


Fig. 8. ESI-MS⁺ (m/z) spectrum for the ultimate catecholase product during the reaction of **1** with 3,5-DTBC.

Herein, we may suggest a plausible mechanism for the catalytic oxidation of 3,5 DTBC to 3,5 DTBQ in presence of air. In the first step of catalytic cycle molecular oxygen take part in the ligand based oxidation reaction of neutral copper complex **1** with redox active di-tertiary butyl substituted phenol based ligand to generate active phenoxyl radical complex species **1a** and simultaneously molecular oxygen is reduced to the H₂O₂. A ligand-centered radical species is most likely responsible for catechol oxidation. Phenoxyl radical complex **1a** (O[•] – Cu^{II} – O[•]) oxidizes 3,5 DTBC to 3,5 DTBQ by capturing two electron from the substrate and itself is transformed to previous

neutral copper complex **1**. If, this oxidation reaction is performed in the presence of a radical scavenger, TEMPO (TEMPO = 2,2,6,6 –tetra methyl piperidinoyl), the formation of quinone is prevented. When catecholase activity of copper complex is monitored in presence of TEMPO, quinone band at 400 nm is not observed spectroscopically. This result suggests that the catechol oxidation catalyzed by Cu (II) complexes is occurred via radical generation [35]. Cyclic voltammetric study supplies additional information of these phenomena.

The di-oxygen of atmosphere is reduced to H_2O_2 during the oxidation process. To detect the formation of hydrogen peroxide during the catalytic reaction we followed the modified iodometric method as indicated in reported paper [17]. Qualitative as well as quantitative detection of I_3^- band (353 nm) by UV- vis spectroscopy is the indication of formation of H_2O_2 during catalytic reaction. The estimation of H_2O_2 clearly indicates that nearly 1 mol of H_2O_2 was shown to be produced per mole of 3,5 DTBC along with 1 mol of 3,5 DTBQ. Such incident clearly suggests that in the catalytic cycle two electron reduction of molecular oxygen is occurred as reported earlier [36].



Scheme 3. A plausible mechanistic pathway for the aerobic catechol oxidation catalyzed by complex **1**.

4. Conclusion

In summary, we have reported a square planar copper(II) complex with a sterically constrained redox active tetradentate phenol based ligand with N_2O_2 donor site. Structure of this compound is characterized by X-ray single crystal diffractometer. A very good agreement between the X-ray and DFT calculated data was obtained. Electronic spectrum calculations of the complex were made by TDDFT/UB3LYP method combined with the SMD solvation in methanol. Comparison of the electrochemical nature of complex **1** with related copper bis phenolate complexes confirms that both the oxidation processes arise due to ligand based oxidation of the phenol moiety to phenoxyl radicals. In addition the copper complex **1** efficiently catalysed the oxidation of 3,5 DTBC to 3,5 DTBQ in presence of air. The turnover number of this reaction is 722 h^{-1} .

Supplementary data

CCDC1861935 contains the supplementary crystallographic data for compound **1**. These data can be obtained free of charge via <http://www.ccdc.cam.ac.uk/conts/retrieving.html>, or from the Cambridge Crystallographic Data Centre, 12 Union Road, Cambridge CB2 1EZ, UK; fax: +44 1223-336-033; or e-mail: deposit@ccdc.cam.ac.uk.

Acknowledgment

Financial support received from Department of Science and Technology, Government of West Bengal, Kolkata (Project memo no. 1071(Sanc)/ST/P/S&T/15G-4/2015 dated 23.02.2016) is gratefully acknowledged. We are grateful for the instrumental support from the Department of Inorganic Chemistry, Indian Association for the Cultivation of Science.

References

1. a) M.C. Linder, C. Goode, *Biochemistry of Copper*, Plenum Press, New York, 1991; (b) Z.Tyeklar, K.D. Karlin, *Acc. Chem. Res.* 22 (1988) 241; c) K. D. Karlin, J. D. Hayes, Y. Gultneh, R. W. Cruse, J. W. McKown, J. P. Hutchinson, J. Zubieta, *J. Am. Chem. Soc.* 106 (1984) 2121; d) R. D.Guiles, J. L. Zimmermann, A. E. V.Mcdermott, A.Yachandra, J. L.Cole, S. L.Dexheimer, R. D.Britt, K.Weighardt, U.Bossek, K.Sauer, M. P. Klein, *Biochemistry* 29 (1990) 471; e) A. M. Wu, J. E. P.Hahn, V. L. Pecoraro, *Chem. Rev.* 104 (2004) 903; f) N.Reddig, D.Pursche,M.Kloskowski, C.Slinn, S. M.Baldeau, A. Rompel, *Eur. J. Inorg. Chem.* (2004) 879; g) E. Ochiai, *Bioinorganic chemistry; An introduction*, Allyn and Bacon, Boston, ch. 9, 1977.
2. (a) E.I. Solomon, D.E. Heppner, E.M. Johnston, J.W. Ginsbach, J. Cirera, M. Qayyum, M.T. Kieber-Emmons, C.H. Kjaergaard, R.G. Hadt, L. Tian, *Chem. Rev.* 114 (2014) 3659; b) R.E. Stenkamp, *Chem. Rev.* 94 (1994) 715; c) R.G. Wilkins, *Chem. Soc. Rev.* 21 (1992) 171; d) N. Kitajima, Y. Moro-oka, *Chem. Rev.* 94 (1994) 737.
3. W. S. Pierpoint, *Biochem. J.* 112 (1969) 609.
4. T. Klabunde, C. Eicken, J. C. Sacchettini, B. Krebs, *Nat. Struct. Biol.* 5 (1998) 1084.
5. a) A. Martinez, I. Membrillo, V. M. Ugalde-Saldivar, L. Gasque, *J. Phys. Chem. B* 116 (2012) 8038; b) B. Sreenivasulu, *Aust. J. Chem.* 62 (2009) 968; c) A. Banerjee, R. Singh, E. Colacio, K. K. Rajak, *Eur. J. Inorg. Chem.* (2009) 277; d) L. Gasque, V. M. Ugalde-Saldivar, I. Membrillo, J. Olguin, E. Mijangos, S. Bernes, I. Gonzalez, *J. Inorg. Biochem.* 102 (2008) 1227; e) A. Banerjee, S. Sarkar, D. Chopra, E. Colacio, K. K. Rajak, *Inorg. Chem.* 47 (2008) 4023; f) I. A. Koval, D. Pursche, A. F. Stassen, P. Gamez, B. Krebs, Jan Reedijk, *Eur. J. Inorg. Chem.* (2003) 1669; g) I. A. Koval, M. Huisman, A. F. Stassen, P. Gamez, O. Roubeau, C. Belle, J. L. Pierre, E. Saint-Aman, M. Lüken, B. Krebs, M. Lutz, A. L. Spek, J. Reedijk, *Eur. J. Inorg. Chem.* (2004) 4036.
6. a) A. L. Abuhijleh, J. Pollitte, C. Woods, *Inorganica Chimica Acta* 215 (1994) 131; b) A. L. Abuhijleh, C. Woods, E. Bogas, G.L. Guenniou, *Inorganica Chimica Acta* 195 (1992) 67; c) M. R. Malachowski, M. G. Davidson, J. N. Hoffman, *Inorganica Chimica Acta* 157 (1989) 91; d) M. R. Malachowski, M. G. Davidson, *Inorganica Chimica Acta* 162 (1989) 199; d) M.

- Mitra, A.K. Maji, B.K. Ghosh, G. Kaur, A.R. Choudhury, C.-H. Lin, J. Ribas, R. Ghosh, *Polyhedron* 61 (2013) 15.
7. a) I. A. Koval, C. Belle, K. Selmeczi, C. Philouze, E. Saint-Aman, A. M. Schuitema, P. Gamez, J. L. Pierre, J. Reedijk, *J. Biol. Inorg. Chem.* 10 (2005) 739; b) J. Reim, B. Krebs, *J. Chem. Soc. Dalton Trans.* (1997) 3793.
 8. a) R. E. H. M. B. Osorio, R. A. Peralta, A. J. Bortoluzzi, V. R. de Almeida, B. Szpoganicz, F. L. Fischer, H. Terenzi, A. S. Mangrich, K. M. Mantovani, D. E. C. Ferreira, W. R. Rocha, W. Haase, Z. Tomkowicz, A. dos Anjos, A. Neves, *Inorg. Chem.* 51 (2012) 1569; b) I. A. Koval, K. Selmeczi, C. Belle, C. Philouze, E. Saint-Aman, I. Gautier-Luneau, A. M. Schuitema, M. van Vliet, P. Gamez, O. Roubeau, M. Lueken, B. Krebs, M. Lutz, A. L. Spek, J.L. Pierre. J. Reedijk, *Chem. Eur. J.* 12 (2006) 6138; c) S. Mukherjee, T. Weyhermueller, E. Bothe, K. Wieghardt, P. Chaudhuri, *Dalton Trans.* (2004) 3842; d) E. Monzani, L. Quinti, A. Perotti, L. Casella, M. Gullotti, L. Randaccio, S. Geremia, G. Nardin, P. Faleschini, G. Tabbi, *Inorg. Chem.* 37 (1998) 553; e) S. Mandal, J. Mukherjee, F. Lloret and R. Mukherjee, *Inorg. Chem.* 51 (2012) 13148; f) A. Neves, L. M. Rossi, A. J. Bortoluzzi, B. Szpoganicz, C. Wiezbicki, E. Schwingel, W. Haase, S. Ostrovsky, *Inorg. Chem.* 41 (2002) 1788; g) A. Biswas, L. K. Das, M. G. B. Drew, C. Diaz and A. Ghosh, *Inorg. Chem.* 51 (2012) 10111.
 9. D. D. Perrin, W. L. F. Armarego, D.R. Perrin, *Purification of Laboratory Chemicals*, Second ed., Peragamon, Oxford, 1980.
 10. G. M. Sheldrick, *SHELXS 97*, *Acta Cryst. A* 46 (1990) 467.
 11. G. M. Sheldrick, *SHELXL 97*. Release 97-1. Program for the Refinement of Crystal Structure, University of Gottingen, Germany, 1997.
 12. Gaussian 09, Revision, M. J. Frisch, G. W. Trucks, H. B. Schlegel, G. E. Scuseria, M. A. Robb, J. R. Cheeseman, G. Scalmani, V. Barone, B. Mennucci, G. A. Petersson, H. Nakatsuji, M. Caricato, X. Li, H. P. Hratchian, A. F. Izmaylov, J. Bloino, G. Zheng, J. L. Sonnenberg, M. Hada, M. Ehara, K. Toyota, R. Fukuda, J. Hasegawa, M. Ishida, T. Nakajima, Y. Honda, O. Kitao, H. Nakai, T. Vreven, J. A. Montgomery, Jr., J. E. Peralta, F. Ogliaro, M. Bearpark, J. J. Heyd, E. Brothers, K. N. Kudin, V. N. Staroverov, R. Kobayashi, J. Normand, K. Raghavachari, A. Rendell, J. C. Burant, S. S. Iyengar, J. Tomasi, M. Cossi, N. Rega, J. M. Millam, M. Klene, J. E. Knox, J. B. Cross, V. Bakken, C. Adamo, J. Jaramillo, R. Gomperts, R. E. Stratmann, O. Yazyev, A. J. Austin, R. Cammi, C. Pomelli, J. W. Ochterski, R. L.

- Martin, K. Morokuma, V. G. Zakrzewski, G. A. Voth, P. Salvador, J. J. Dannenberg, S. Dapprich, A. D. Daniels, Ö. Farkas, J. B. Foresman, J. V. Ortiz, J. Cioslowski, and D. J. Fox, Gaussian, Inc., Wallingford CT, (2009).
13. a) A. D. Becke, *J. Chem. Phys.* 98 (1993) 5648; b) C. Lee, W. Yang, R.G. Parr, *Phys. Rev. B* 37 (1988) 785.
 14. P. J. Hay and W. R. Wadt, *J. Chem. Phys.* 82 (1985) 270.
 15. J. Mukherjee, R. Mukherjee, *Inorg. Chim. Acta.* 337 (2002) 429.
 16. F. Zippel, F. Ahlers, R. Werner, W. Haase, H. F. Nolting, B. Krebs, *Inorg. Chem.* 35 (1996) 3409.
 17. a) M. Das, R. Nasani, M. Saha, S. M. Mobin, S. Mukhopadhyay, *Dalton Trans.* 44 (2015) 2299; b) A. I. Vogel, *A Text Book of Quantitative Inorganic Analysis*, Third ed., Wiley, New York (1961) p. 343.
 18. K. Nakamoto, *Infrared and Raman Spectra of Inorganic and Coordination Compounds*, Third ed., Wiley-Inter-science, New York, 1978.
 19. a) D. Mandal, S.K.T. Abtab, A. Audhya, E.R.T. Tiekink, A. Endo; R. Clerac, M. Chaudhury, *Polyhedron* 52 (2013) 355; b) D. Mandal, P. B. Chatterjee, S. Bhattacharya, K. Y. Choi, R. Clerac, M. Chaudhury, *Inorg. Chem.* 48 (2009) 1826; c) B. Mandal, T. Chakraborty, I. Ali, D. Mondal, M. C. Majee, S. Raha, K. Ghosh, P. Mitra, D. Mandal, *J. Indian Chem. Soc.* 94 (2017) 1079; d) D. Mandal, S. Raha, T. Rakshit, A. D. Das, K. C. Ghosh, P. Mitra, *J. Environ. & Sociobiol.* 13 (2016) 15.
 20. a) R. Vafazadeh, R. Esteghamat-Panah, A. C. Willis, A. F. Hill, *Polyhedron* 48 (2012) 51; b) P. A. N. Reddy, M. Nethaji, A. R. Chakravarty, *Inorganica Chimica Acta* 337 (2002) 450; c) M. Devereux, D. O Shea, A. Kellett, M. McCann, M. Walsh, D. Egan, C. Deegan, K. Kedziora, G. Rosair, H. Muller-Bunz, *J. Inorg. Biochem.* 101 (2007) 881.
 21. A. W. Addison, T. N. Rao, J. Reedijk, J. van Rijn, G. C. Verschoor, *J. Chem. Soc. Dalton Trans.* (1984) 1349
 22. L. Yang, Douglas R. Powell, R. P. Houser *J. Chem. Soc. Dalton Trans.* (2007) 955.
 23. A. B. P. Lever, *Inorganic Electronic Spectroscopy*, Second ed., Elsevier Science, The Netherlands, 1984.

24. a) D. X. West, A. E. Liberta, S. B. Padhye, R. C. Chikate, P. B. Sonawane, A. S. Kumbhar, R. G. Yerande, *Coord. Chem. Rev.* 123 (1993) 49; b) S. S. Konstantinovic, B. Radovanovic, Z. Cakic, V. Vasic, *J. Serb. Chem. Soc.* 68 (2003) 641; c) B. Mandal, A. Mondal, T. Rakshit, M. C. Majee, S. Raha, M. Paramanik, P. Mitra, D. Mandal, *J. Indian Chem. Soc.* 95 (2018) 1029.
25. (a) A. John, Mobin M. Shaikh, P. Ghosh *Dalton Trans.* (2008) 2815; (b) Y. Shimazaki, F. Tani, K. Fukui, Y. Naruta, O. Yamauchi, *J. Am. Chem. Soc.* 125 (2003) 10512.
26. a) J. B. H. Strautmann, S. D. George, E. Bothe, E. Bill, T. Weyhermüller, A. Stämmler, H. Bögge, T. Glaser, *Inorg. Chem.* 47 (2008) 6804; b) J. B. H. Strautmann, C. G. F. Richthofen, G. H. Brückner, S. DeBeer, E. Bothe, E. Bill, T. Weyhermüller, A. Stämmler, H. Bögge, T. Glaser, *Inorg. Chem.* 50 (2011) 155.
27. A. K. Nairn, S. J. Archibald, R. Bhalla, B. C. Gilbert, E. J. MacLean, S. J. Teat, P. H. Walton, *Dalton Trans.* (2006) 172.
28. H. Arora, C. Philouze, O. Jarjayes, F. Thomas, *J. Chem. Soc. Dalton Trans.* 39 (2010) 10088
29. S. Adhikari, A. Banerjee, S. Nandi, M. Fondo, J. Sanmartín-Matalobos, D. Das, *RSC Adv.* 5 (2015) 10987.
30. M. K. Panda, Mobin M. Shaikh, R. J. Butcher, P. Ghosh, *Inorganica Chimica Acta* 372 (2011) 145.
31. S. Caglar, I. E. Aydemir, E. Adıgüzela, B. Caglar, S. Demirb, O. Buyukgungo, *Inorganica Chimica Acta* 408 (2013) 131.
32. A. Neves, L. M. Rossi, A. J. Bortoluzzi, B. Szpoganicz, C. Wiezbicki, E. Schwingel, *Inorg. Chem.* 41 (2002) 1788.
33. S. Mandal, J. Mukherjee, F. Lloret, R. Mukherjee, *Inorg. Chem.* 51 (2012) 13148.
34. A. Biswas, L. K. Das, M. G. B. Drew, C. Diaz, A. Ghosh, *Inorg. Chem.* 51 (2012) 10111.
35. A. Guha, T. Chattopadhyay, N. D. Paul, M. Mukherjee, S. Goswami, T. K. Mondal, E. Zangrando, D. Das, *Inorg. Chem.* 51 (2012) 8750.
36. A. Hazari, L. K. Das, R. M. Kadam, A. Bauzá, A. Frontera, A. Ghosh, *Dalton Trans.* 44 (2015) 3862.

A square planar copper(II) complex with a sterically constrained redox active tetradentate phenol based ligand with N_2O_2 donor site have been prepared. Structure of this compound is characterized by X-ray single crystal diffract meter. Comparison of the electrochemical nature of complex **1** with related copper bis phenolate complexes confirms that both the oxidation processes arise due to ligand based oxidation of the phenol moiety to phenoxyl radicals. The copper complex **1** efficiently catalysed the oxidation of 3,5 DTBC to 3,5 DTBQ in presence of air. The turnover number of this reaction is 722 h^{-1} .

Highlights

- The mononuclear complex of general formula $[\text{Cu}^{\text{II}}\text{L}]$ was prepared.
- The structure of the complex was characterized by single crystal X-ray crystallography and various spectroscopic tools.
- Geometries of ground state for the complex were optimized by density functional theory.
- Catechol oxidase activity of the complex was performed.